ASSESSMENT OF OPTICAL TRANSCEIVER COMPATIBILITY OF THE MUON BACKEND SYSTEM FOR THE CMS EXPERIMENT AT THE LHC

An Undergraduate Research Scholars Thesis

by

SHACHAR GOTTLIEB

Submitted to the LAUNCH: Undergraduate Research office at
Texas A&M University
in partial fulfillment of requirements for the designation as an

UNDERGRADUATE RESEARCH SCHOLAR

Approved by
Faculty Research Advisor: Dr. Alexei Safonov

May 2023

Major: Physics

RESEARCH COMPLIANCE CERTIFICATION

Research activities involving the use of human subjects, vertebrate animals, and/or biohazards must be reviewed and approved by the appropriate Texas A&M University regulatory research committee (i.e., IRB, IACUC, IBC) before the activity can commence. This requirement applies to activities conducted at Texas A&M and to activities conducted at non-Texas A&M facilities or institutions. In both cases, students are responsible for working with the relevant Texas A&M research compliance program to ensure and document that all Texas A&M compliance obligations are met before the study begins.

I, Shachar Gottlieb, certify that all research compliance requirements related to this Undergraduate Research Scholars thesis have been addressed with my Faculty Research Advisor prior to the collection of any data used in this final thesis submission.

This project did not require approval from the Texas A&M University Research Compliance & Biosafety office.

TABLE OF CONTENTS

Page

ABSTRACT

Assessment of Optical Transceiver Compatibility of the Muon Backend System for the CMS Experiment at the LHC

Shachar Gottlieb
Department of Physics and Astronomy
Texas A&M University

Faculty Research Advisor: Dr. Alexei Safonov
Department of Physics and Astronomy
Texas A&M University

The Large Hadron Collider (LHC), the largest particle accelerator in the world, is planning on upgrading its performance in the upcoming High-Luminosity LHC project. This project will increase the flux of incoming particles in the detectors and the rate of data collection, seeking to reveal new elements of physics related to the Standard Model and beyond. To accomplish this upgrade, the electronics in the LHC detectors must be improved to handle the higher rate of data. As part of this upgrade, the Compact Muon Solenoid (CMS) experiment, a general-purpose detector and one of the four main experiments at the LHC, seeks to use new high-speed optical transceivers. These transceivers will be essential for fast and reliable transmission of large amounts of data between the frontend muon detector interfaces and backend processing systems of the CMS muon system. This research study seeks to verify that these optical transceivers will meet the specifications for reliable operation in the CMS experiment by checking their compatibility with the design of the backend system and the

multiple interface systems that the backend will interact with. A testing procedure has been created for qualification of the optical transceivers, and involves testing a chosen sample of transceivers using different muon frontend components and determining the optical signal strength at which they begin to fail. This testing procedure will allow validation of the design of the backend system and will prove whether or not all optical transceiver devices satisfy the required specifications.

ACKNOWLEDGEMENTS

Contributors

I would like to thank my faculty advisors, Dr. Alexei Safonov and Dr. Jason Gilmore, for their guidance and support throughout the course of this research. I would also like to thank Evaldas Juska for providing assistance during the course of this research project.

Thanks also go to my friends and colleagues Ali Ahmad, Kyla Martinez, and Jessica Williams for their assistance during this project.

The materials analyzed for Assessment of Optical Transceiver Compatibility of the Backend System for the CMS Experiment at the LHC were provided by the CMS group. The analyses depicted in Assessment of Optical Transceiver Compatibility of the Backend System for the CMS Experiment at the LHC were conducted by Shachar Gottlieb and the data used is unpublished.

All other work conducted for the thesis was completed by the student independently.

Funding Sources

Undergraduate research was supported by Texas A&M University. This work was also made possible in part by CMS. Its contents are solely the responsibility of the authors and do not necessarily represent the official views of CMS.

NOMENCLATURE

CERN	European Organization for Nuclear Research
LHC	Large Hadron Collider
HL-LHC	High-Luminosity Large Hadron Collider
CMS	Compact Muon Solenoid
QSFP	Quad Small Form-Factor Pluggable optical transceivers
X2O	Custom-built modular ATCA card
GEM	Gas Electron Multiplier muon detector type
CSC	Cathode Strip Chamber muon detector type
ME0	Muon Endcap 0, GEM type interface
GE2/1	GEM Endcap Station 2 Ring 1, GEM type interface
DMB	Data Mother Board, CSC type interface
VTRX	Versatile Link Transceiver
BER	Bit Error Rate
PRBS	Pseudorandom Binary Sequence
Sensitivity	Weakest optical signal at which device works reliably
VOA	Variable Optical Attenuator
OPM	Optical Power Meter
FEC	Forward Error Correction

1. INTRODUCTION

1.1 Large Hadron Collider

The Large Hadron Collider (LHC) is the world’s largest particle accelerator, and the particle accelerator capable of highest energy collisions in the world. The LHC was built by the European Organization for Nuclear Research (CERN) and is located in Geneva, Switzerland [2]. The LHC accelerator is built in a circular underground tunnel with a circumference of 27 kilometers, and has four main detector experiments – CMS, ATLAS, ALICE, and LHC-B – seen in Figure 1. The LHC accelerates bunches of protons to energy of 7 TeV and collides them at a rate of 40 million collisions per second. The LHC then uses detectors to observe these resulting high energy proton-proton collisions and make precision measurements to study the most energetic collisions, in order to improve measurements of the Standard Model and discover phenomena not described by the Standard Model.

The Standard Model of particle physics is a framework accurately describing much of the subatomic world, including all known fundamental particles and three of the four fundamental forces [3]. The model divides all known particles into several categories, namely quarks, leptons, and bosons. Quarks and leptons are matter particles; for example, protons and neutrons are composite particles made of quarks, while electrons and muons are leptons. Bosons, on the other hand, are force carrier particles – including photons which carry the electromagnetic force, W and Z bosons which carry the weak force, gluons which carry the strong force. Another example of a particle is the Higgs boson, a particle discovered in 2012 by two of the LHC’s experiments, CMS and ATLAS. The Higgs field permeates space and provides elementary particles with mass via their interactions with the field.

However, the Standard Model also has certain limitations and incomplete parts. Precision measurements of high energy particle collisions may allow discovery of new physics related to the Standard Model, such as the existence of the graviton – the theoretical particle responsible for the gravitational force, which in certain scenarios can be discoverable at the LHC. Continued high energy measurements in the LHC may lead to findings beyond the Standard Model, such as the discovery of dark matter or supersymmetry [4].

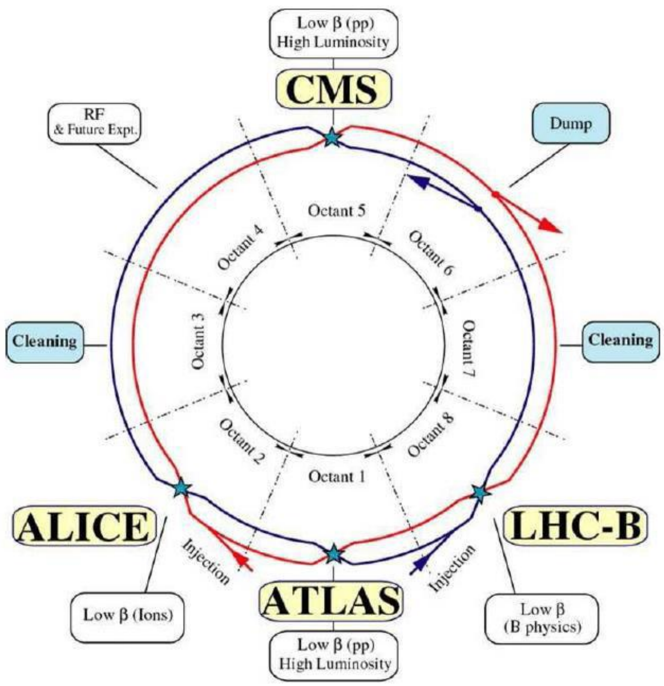

Figure 1: Diagram of the Large Hadron Collider particle accelerator, with the four main experiments shown in yellow. [7]

1.2 Compact Muon Solenoid

The Compact Muon Solenoid (CMS) is one of the four main experiments conducted in the Large Hadron Collider [1], and one of the LHC's two general-purpose detectors. It has multiple systems capable of measuring the properties of the resulting particles from the proton-proton collisions occurring in its interaction point.

The CMS detector has multiple sub-detector layers, seen in Figure 2 and Figure 3 [8]. The particles from the collisions pass through a silicon tracker layer, which identifies the tracks of all charged particles. Next they pass through the Electromagnetic Calorimeter layer, which measures the energies of photons and electrons as they are captured by the detector. Similarly, the Hadron Calorimeter layer measures the energies of hadrons (protons, neutrons, etc.) and stops them from passing through. The only particles (with the exception of neutrinos) that pass through to the outer layer are the muons; these particles are then identified and measured in the muon chambers of the muon system, an integral part of the CMS experiment. A powerful solenoid is present in the detector, which acts on all charged particles, such as the muons. The magnetic field from the solenoid bends the track of the muons - the bends in the tracks being proportional to the muons' transverse momentum..

Muons are types of fundamental particles in the Standard Model similar to electrons: they are leptons and carry the same charge, but have over 200 times the mass of the electron, which enables them to pass through a lot of matter without stopping [10]. By measuring these high energy muons, more measurements of the Higgs bosons and other rare processes can be performed and new discoveries beyond the Standard Model can be investigated.

In nature, muons typically come from decay of cosmic rays in the atmosphere of the earth and proceed to shower down to the surface. Muons have a lifetime of only 2.2 microseconds, but due to their relativistic velocities they are capable of reaching the surface of the earth from the upper atmosphere.

In the CMS detector, muons have four primary sources: decay from light flavor bound states, heavy flavor decays, decays from W, Z, and Higgs bosons, and rarely hadrons misidentified as muons. In particular, the decay of Higgs bosons to muons is one process of interest, as Higgs bosons can’t be directly observed due to their very short lifetime.

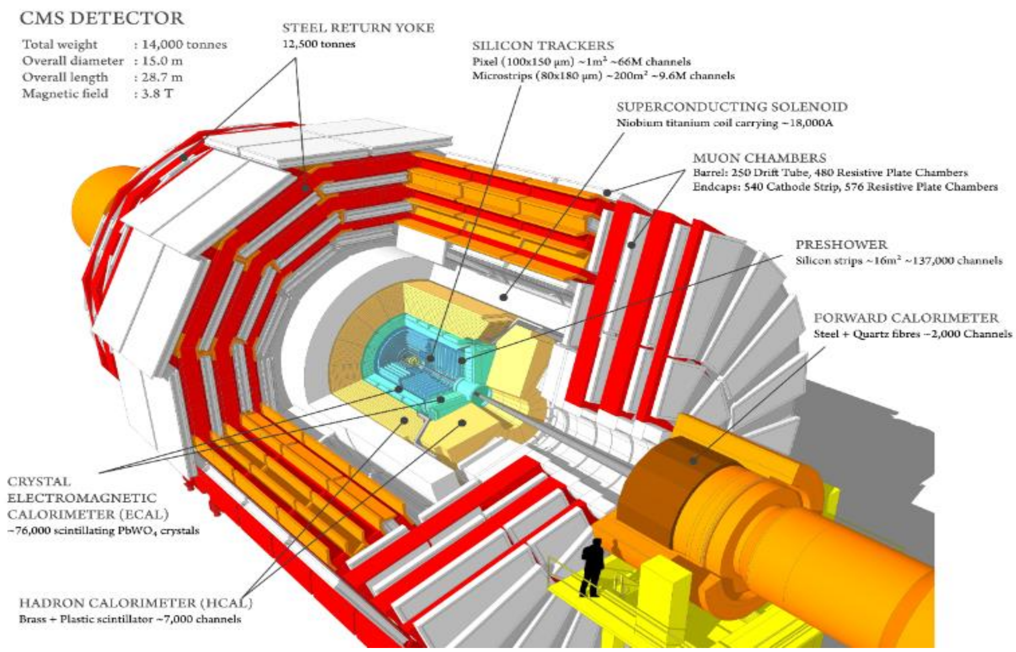

Figure 2: Compact Muon Solenoid detector, consisting of silicon trackers, electromagnetic and hadron calorimeters, the solenoid, and the muon system [8]

1.3 Endcap region

The muon system has two main detection regions, the barrel and endcap region, seen in Figure 3. The barrel region has two types of muon detectors, called Drift Tubes (DT) and Resistive Plate Chambers (RPC). The endcap region has a few different types of muon detectors: Gas Electron Multipliers (GEM), Cathode Strip Chambers (CSC), and RPCs.

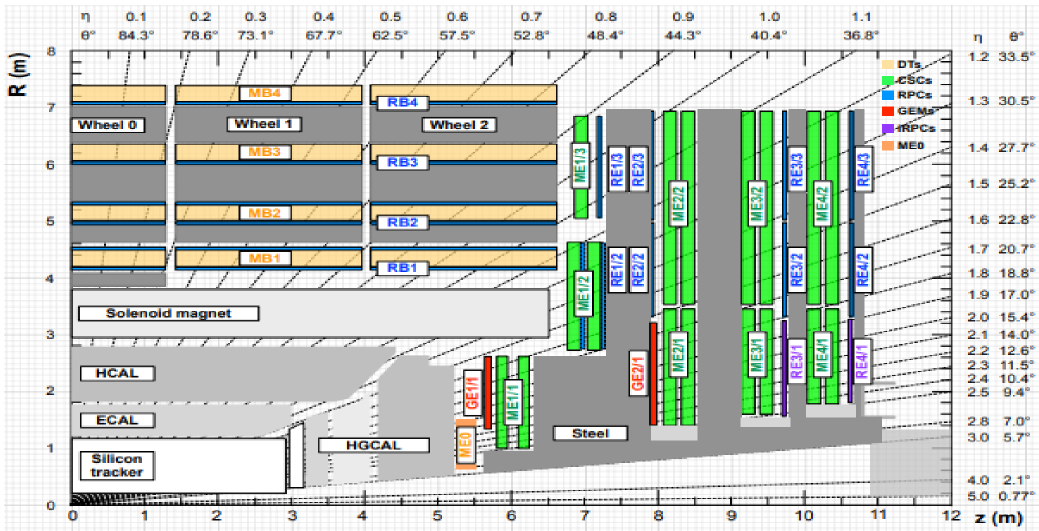

Figure 3: Layers and muon system of the CMS experiment. Gas Electron Multipliers (GEM) are shown in red and Cathode Strip Chambers (CSC) in green.

Two detector types in particular are studied in this research: the GEM and CSC interface systems. A diagram of a CSC type interface can be seen in Figure 4 - these interfaces are constructed of multiple detector layers with gas in between. The CSC detectors and the ME0 version of the GEM detectors all have 6 detector layers; All other GEM versions have only 2 layers.

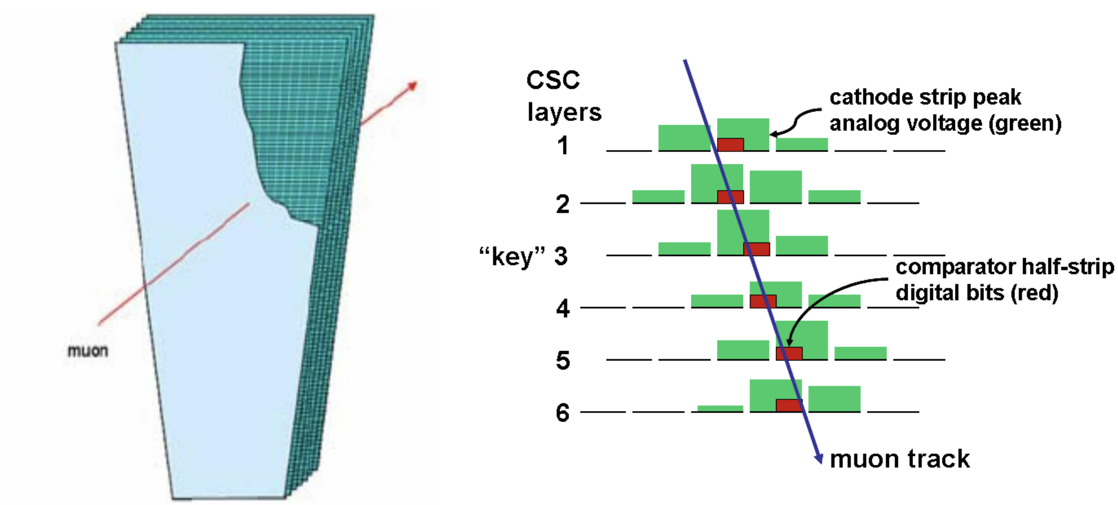

Figure 4: Diagram of CSC detector with 6 layers and a muon passing through; muon track can be reconstructed using hits on each layer of the detector. [13] [11]

When a muon passes through the gas in a chamber it ionizes the gas, causing generation of free electrons. As they accelerate in the electric field this leads to a cascade of electrons, which are then detected as a sudden pulse of charge by cathode strips on the detector interfaces. Each layer of the detector records the location of the strip and wire that detected the charge, essentially the x and y coordinates where the muon passed through. By using the locations from all the layers, a muon track can be reconstructed, which reveals the path of the muon as well as a measurement of its momentum.

This data is then transmitted over high-speed optical links to the backend electronics processing system and to a special electronics system referred to as the Level 1 (L1) Trigger [12]. Millions of particle collisions occur every second in the detector, which corresponds to terabytes of information being collected every second. It is impossible to store all of this data; as such, the L1 Trigger system is responsible for fast and efficient identification and tagging of data which contains the most interesting physics events. This chosen data is kept for more detailed analysis later, and all other data is discarded.

1.4 High-Luminosity LHC

The High-Luminosity LHC (HL-LHC) is an accelerator upgrade project aiming to increase the luminosity of the LHC – the rate of collisions in the detector – by a factor of ten. There is a corresponding upgrade for the CMS detectors to handle the increase in data, and this work is planned to start in 2025, with operation planned for 2029 [5]. One such improvement will be to the muon system, which must upgrade its detectors and the L1 Trigger system.

One of the requirements of this upgrade is to the optical link system which transmits data between the frontend muon detector interfaces and the L1 Trigger system. This system must be able to transmit the large amounts of information fast enough for the L1 Trigger system to have time to analyze it – this requires hundreds of new high-speed optical transceivers.

1.5 Optical Transmission

Attenuation occurs in optical fibers over long distances of data transmission, meaning there is a signal loss throughout the fiber due to light scattering and absorption. Other factors, such as radiation damage and fiber interface penalties, may also affect the optical signal.

Weak optical signals can lead to errors in the data during transmission. Such errors are unwanted, so extensive testing of the optical transceivers connected to the optical fibers is required to ensure their working condition, even with weakest optical signals.

This research focuses on testing these new optical transceivers, produced by different manufacturers, with every combination of GEM and CSC interfaces, as well as a custom-made processing board that is part of the backend system. This testing involves identifying the maximum sensitivity of the optical transceivers – meaning the weakest optical signal at which they reliably satisfy working specifications.

2. METHODS

2.1 Electronics

The launch of the HL-LHC project will increase the rate of data being collected by the CMS experiment, requiring new and improved electronics to transmit the data from the muon system and process it.

One of the new electronics used is a modular Advanced Telecommunications Computing Architecture (ATCA) card called the X2O, which is a custom-made electronics board with the purpose of being used to quickly receive and process data received from the frontend interfaces. To communicate with the frontend interfaces, the X2O has an optical module with 30 cages suitable for Quad Small Form-Factor Pluggable (QSFP) optical transceivers used for data transfer; these cages can be seen in Figure 5, which shows the ATCA crate test stand used at TAMU, accompanied by two of the QSFP types plugged into these cages.

QSFPs are optical transceivers with four optical receiver (RX) and four optical transmitter (TX) channels. They are capable of a high rate of data transmission, with the ones tested at TAMU either being QSFP+ devices capable of 10 gigabit per second (Gbps) communication per channel or QSFP28 devices capable of 25 Gbps communication per channel. In the testing setup used, these QSFPs are connected to optical fibers originating from the frontend detector interfaces and passing multiple optical devices used in the testing of each QSFP's optical sensitivity.

In the testing performed at TAMU, three different types of frontend interfaces were tested: the GE2/1 and ME0, which are types of GEM detector interfaces, and the Data Mother Board (DMB), which is a type of CSC interface. These frontend interfaces have optical transceivers on them to transmit and receive data from the QSFPs on the X2O. On the GE2/1, these transceivers are called Versatile Link Transceivers (VTRX), and similarly on the ME0 the transceivers are called VTRX+, both of which are rad-hard optical devices manufactured by CERN. On the DMB, these transceivers are called Firefly, which are commercial optical devices manufactured by Samtec.

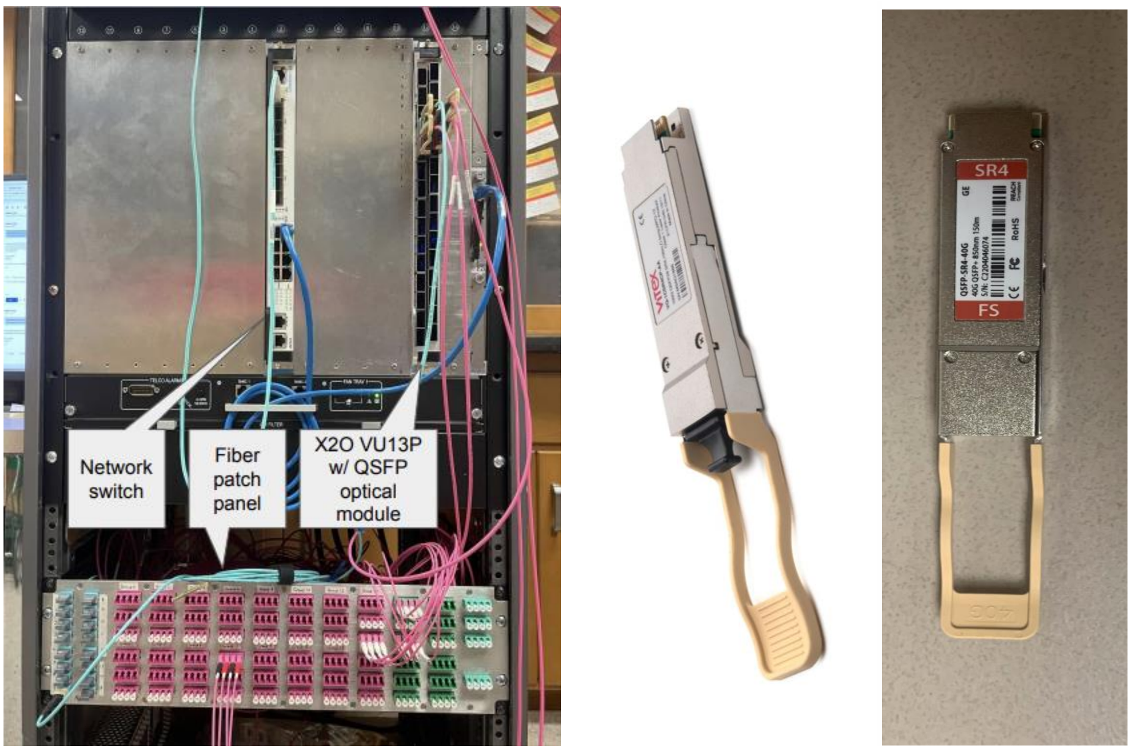

Figure 5: Left: ATCA crate at TAMU. Middle: Vitex QSFP+ [6]. Right: FS QSFP+ [14]

2.2 Test Validation

One of the main goals of this research project is to ensure that QSFPs pre-selected for the CMS experiment are able to transmit data reliably and meet the specific requirements of the CMS environment. When testing these QSFPs, attenuation of the fibers due to a multitude of factors has to be taken into account. This attenuation causes the optical power of light passing through the fibers to weaken, possibly leading to failures in the data during transmission. To determine whether or not the QSPFs will work, each QSFP's optical receiver sensitivity – the minimum optical power at which the QSFP operates reliably – is measured to see if the sensitivity is compatible with the weakest incoming signal expected to occur. In Figure 6, various factors were taken into account that could lower the optical power transmitted from the ME0 or GE2/1 interfaces during real data collection in the CMS experiment. These factors include: the worst-case possible output by the VTRX+ and VTRX transceivers, fiber damage over time due to radiation, link penalties(including chromatic dispersion, mode partition and modal noise, and reflection noise), attenuation of the fibers, and an additional forward error corrected (FEC) margin of 2 decibel-milliwatt (dBm).

Based on all of these attenuation factors, the cutoff for which it is decided if a QSFP works or not was decided to be at a signal strength of -11 dBm, with a bit error rate (BER) of less than 10^{-12}; meaning that when the QSFP is receiving an optical signal with a magnitude of -11 dBm, it is considered to be working if less than 1 out of every 10^{12} bits has an error. Bit errors are defined as the number of received bits in a binary sequence that do not match the bit sequence originally sent from the transmitter.

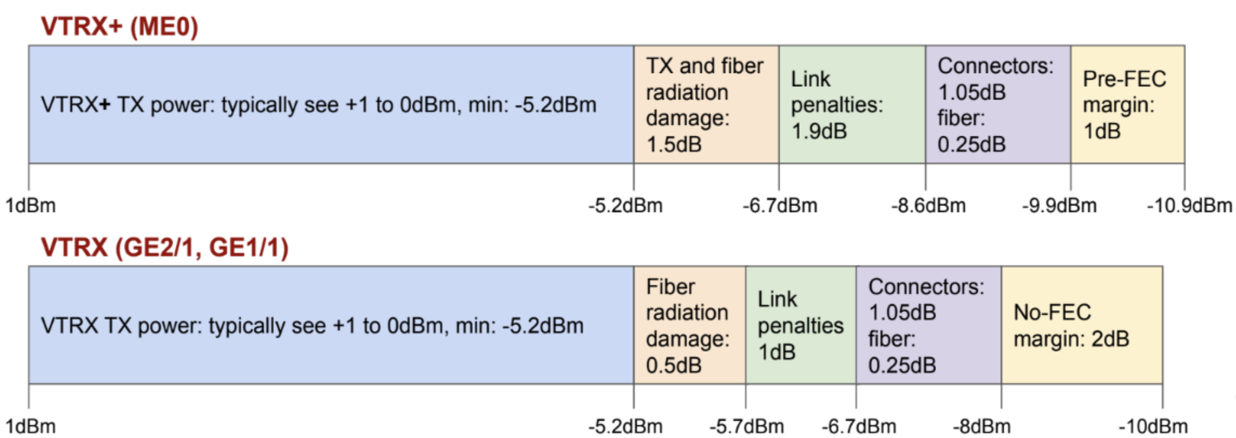

Figure 6: VTRX and VTRX+ expected worst-case optical transmission power budget

Another purpose of this testing is to decide which QSFP type is best suited to be used in the CMS experiment. QSFPs from three different manufacturers were used in the experiments performed: Vitex [6], FS [14], and Addon. To test a significant number of QSFPs, 40 parts were received from both the Vitex and FS vendors to be tested.

2.3 Automatic Testing Setup

A testing procedure and test stand were created at TAMU to automatically test the many QSFPs to ensure they meet the previously defined standard of a BER less than 10^{-12} at a sensitivity of -11 dBm. The testing procedure was created such that it replicates as best as possible the working conditions of the system at the CMS experiment during the actual run of the HL-LHC.

In order to evaluate the QSFP performance without real data from the muon detectors, a digital loopback is run by the X2O using a pseudorandom binary sequence(PRBS), meaning that the X2O generates randomized sequence of bits, sends them through the QSFP to the frontend interface, then returns the binary sequence back to the X2O, which then receives the sequence and compares it to the original PRBS and counts the number of bit errors during transmission.

Several electronic components are used at the test stand built at TAMU to determine the sensitivity of each QSFP, as can be seen in Figure 7 and Figure 8. Starting with the signal coming from any frontend interface, the signal will then travel through the variable optical attenuator (VOA). The VOA is a programmable tool that is capable of decreasing the strength of the optical signal in a precise way. This allows control of the amount of power that will be received by the QSFP, which is used to determine its sensitivity by gradually decreasing the optical power until the test fails. Next, an optical switch is used, where our custom software is used to switch between four different fibers which lead to different optical channels for the test.

The switch is connected to the optical power meter (OPM) and three of the four QSFP channels, allowing automatic testing of three channels consecutively by switching between them using our custom software tools. The optical power meter is capable of measuring the magnitude of the signal, which is used to identify the sensitivity of each QSFP channel.

All of these components are controlled by a Raspberry Pi, using different connection methods of I2C, GPIO, and USB for the VOA, optical switch, and OPM, respectively, as detailed in Figure 7. This allows automated control of these three parts through software run on the Raspberry Pi's Linux operating system. In the testing procedure used at TAMU, a desktop PC is used to run the entire test, by coordinating communications between the Raspberry Pi and the X2O. In this way the software controls the scan through attenuation levels with loops over all the separate components required for determining the QSFP's sensitivity.

The code used to control this entire system of components was written and developed by the TAMU CMS group specifically for use in testing of QSFPs. The program is described in more detail in the next section, the testing procedure.

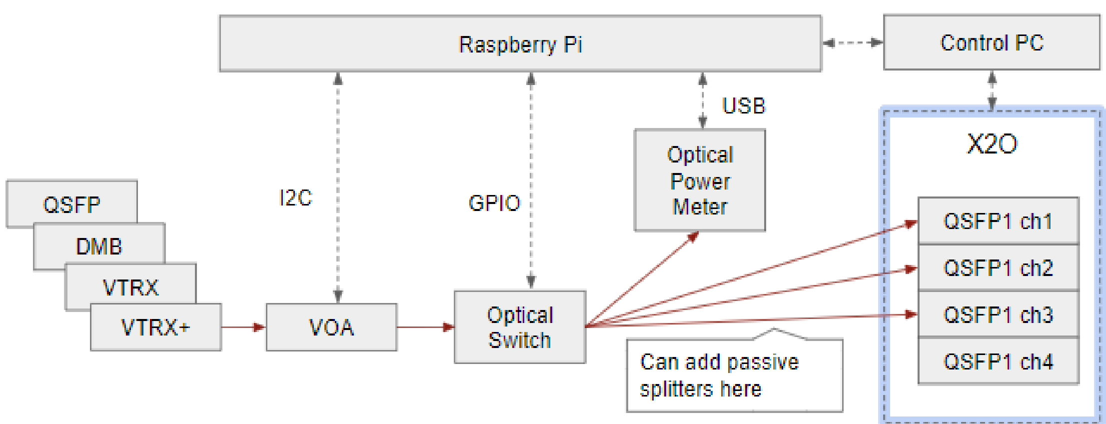

Figure 7: Diagram of test stand components, which includes a Variable Optical Attenuator (VOA), Optical Switch, and Optical Power Meter)OPM), as well as the QSFPs and frontend optical components from the CMS muon system.

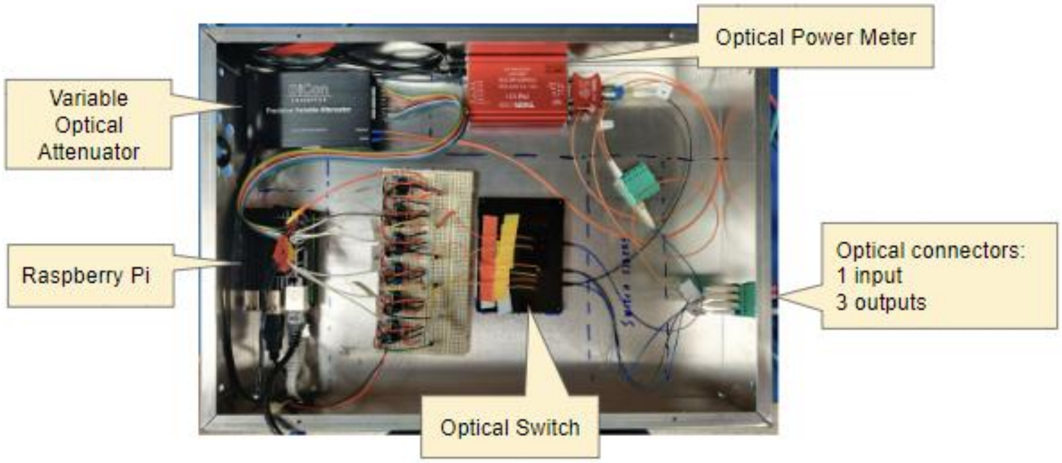

Figure 8: Picture of the optical components installed in the test stand built at TAMU

2.4 Testing Procedure

To test a QSFP transceiver, the chosen QSFP has to be plugged into one of the X2O optical module cages in Figure 5. In the testing performed at TAMU, the cage used to test all QSFPs is cage #8, with the numbering starting at cage 0 on the top right. Then, the frontend interface being tested together with the QSFP has to be connected to the X2O: an input fiber is inserted in the input optical connector slot shown in Figure 8, and for the GEM detectors an output fiber is connected to the fiber patch panel shown in Figure 5.

The X2O FPGA module also has to be programmed to work with each frontend interface, which can be done by connecting to the X2O using a Linux terminal and running the firmware loading script corresponding to the interface used. Communication servers are then run on the X2O and Raspberry Pi, which allow the desktop PC to access scripts on the two devices and thereby remotely control all the electronics and run the entire test algorithm.

Algorithm 1 below outlines the testing method used for each QSFP. Initially, a command specifying the program to run, then the QSFP ID and a source ID are input as arguments when running the script on a Linux operating system . The QSFP ID identifies the QSFP manufacturer

– Vitex, FS, or Addon – and a number assigned to each QSFP. The source ID identifies the interface used, which is important because each interface has a different rate of data transmission and optical power output, which affects the time for test completion and the final sensitivity of the QSFP.

Typically, an optimized test run with the frontend interface with highest transmission speed, the ME0, takes about half an hour to finish finding the maximum sensitivity for all three channels of one QSFP. Similarly, for the GE2/1 and DMB interfaces which are about twice and four times as slow as the ME0, respectively, the testing time for one QSFP is about an hour or two to find the sensitivity for all three channels. This requires the software written to be as efficient as possible, to minimize the time it takes to test all QSFPs.

After these arguments are set in the code, the computer connects to the X2O and Raspberry Pi, as well as the VOA, OPM, and optical switch. Next, a preliminary test is performed to optimize the program – it performs a quick scan with only 10^{10} bits sent. This testing is done by continuously sending a bitstream from the X2O and looping it for the duration of time it takes each interface to send that number of bits. Whenever the test passes with less than 2 bit errors, the attenuation is increased by a defined step size, thus decreasing the received power each time. This is done continuously until more than 2 errors occur, at which point the last working attenuation level is saved. This allows an estimate to the point at which full testing should be done, to optimize testing time.

The full test is then used. Using statistical calculations, it was determined that requiring at most 1 bit error in 10^{12} bits at 95% confidence level would be equivalent to observing less than 2 errors in $4.75*10^{12}$ bits, which is the method used in this algorithm. For the full test, the attenuation is gradually decreased, until less than 2 errors occur. To increase the efficiency of the algorithm, if at least 2 errors are found during one attenuation step, this is a clear indication of a weak signal, so the software skips to the next attenuation step to save time.

Once the ultimate point with less than 2 errors has been found, the OPM is used to measure the optical power at that attenuation level, which is defined as the QSFP's sensitivity for the channel tested. This value is printed and a log file of all attenuation steps is saved. This process is then repeated for all three channels being tested on each QSFP.

Algorithm 1: QSFP testing algorithm

```
Input: Command, QSFP ID, Source ID
Output: For each QSFP channel, value of sensitivity and a log file
Define bitrate and initial attenuation based on source type
Configure connections to X2O and Raspberry Pi
for each QSFP channel
    while errors ≤ 1
        Perform a fast preliminary test, starting at initial attenuation and increasing the
        attenuation in steps
        Record number of errors and optical power at each step
    while errors ≥ 1
        Perform full sensitivity testing, starting at last attenuation of the preliminary test
        and decreasing the attenuation in steps
        Record number of errors and optical power at each step
    End
    Print optical power value
    Save log file of all attenuation steps taken
End
```

3. RESULTS

To prove which QSFPs are compatible with the X2O and meet the specifications, a large number of QSFPs have been tested using the test stand at TAMU. This testing included multiple different QSFP types, features, and interface systems.

These optical transceivers were tested using an algorithm with enough statistical significance using $4.75*10^{12}$ bits, such that there is a 95% level of confidence of these devices working as intended with less than a 10^{-12} bit error rate at an attenuation level of -11 dBm or lower. The uncertainty of each sensitivity measurement of a QSFP was set to be in 0.1 dBm, and there is an additional uncertainty in the reading every time the same QSFP is re-plugged into the X2O due to slight differences in the configuration of the connection. These may lead to slight differences between QSFPs in testing and in retesting of the same QSFP. Additional factors, such as dust potentially on the optical connections in the testing setup, may also lead to differences in testing.

For the ME0, GE2/1, and DMB interfaces tested, all QSFPs used were capable of 40 Gbps transmission, or 10 Gbps for each of the four channels. Due to the fact that only three optical switch ports were available for use in the automatic testing, with the fourth used for connecting to the optical power meter, only three of the four receiver channels of each QSFP were tested. These channels tested were numbered 0, 2, and 3, and were prefixed with “GBT” when tested using the GEM type interfaces (for example GBT-0), or with “DMB” for CSC type interfaces.

3.1 QSFP Manufacturers

One of the objectives of this research study was to determine which of several different QSFP types would be most suitable for use in the CMS experiment. QSFPs from two different manufacturers were primarily used in this testing: Vitex and FS type QSFPs. Forty different QSFPs of each type were tested using the ME0 interface, which can be seen in Figure 9.

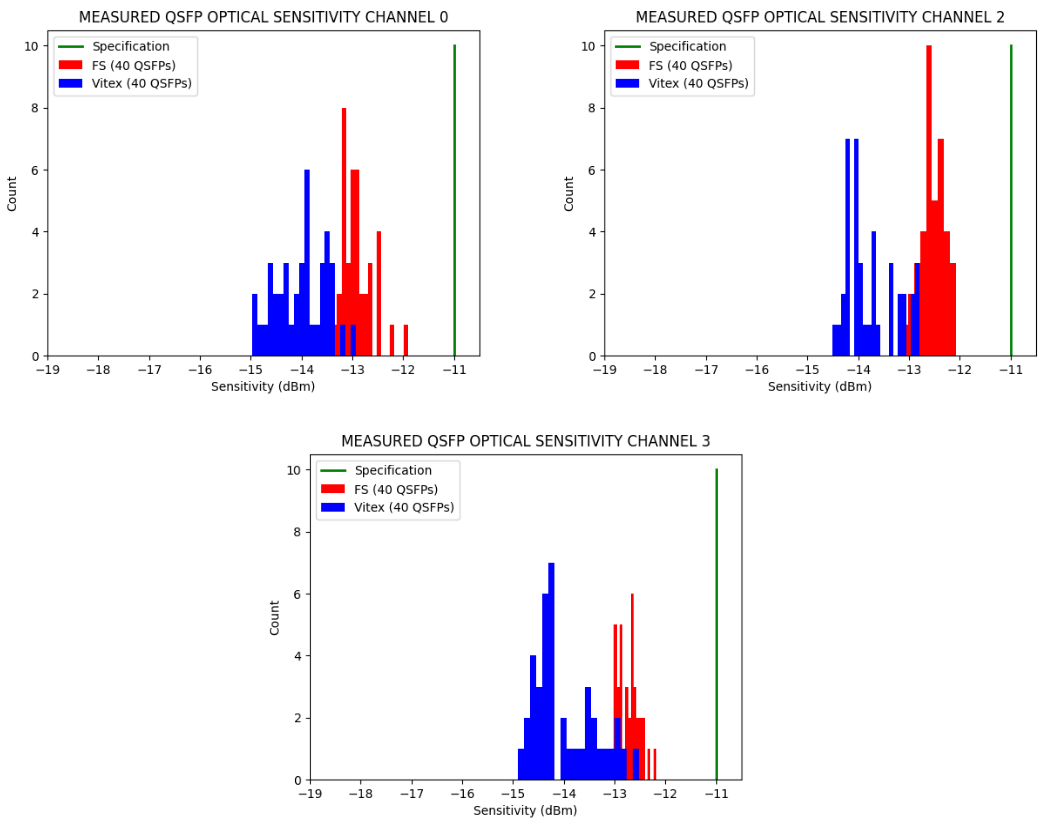

Figure 9: Comparisons of sensitivities measured using 40 different FS and Vitex QSFPs, the charts representing channels 0, 2, and 3 of the QSFPs, respectively. Sensitivity smaller than -11 dBm meets our design specification for use in CMS.

The three plots correspond to the three channels tested for each QSFP, numbered 0, 2, and 3, respectively from left to right, top to bottom. The x-axis represents the maximum receiver sensitivity measurement of each QSFP, measured in decibel-milliwatt (dBm), commonly used in fiber-optic communication.

The red histogram represents the FS QSFPs tested, and the blue histogram represents the Vitex QSFPs tested. The green line is the minimum specification which QSFPs must surpass to be deemed compatible with the requirements for use in the CMS muon system. In this case, weaker sensitivities indicate better testing results, so tested measurements must be to the left of the green line.

Two QSFPs from a third manufacturer, Addon, were also tested; the results of which are shown in Table 1.

Table 1: Sensitivities of two Addon QSFPs tested

Addon QSFP Sensitivity	GBT-0 (dBm)	GBT-2 (dBm)	GBT-3 (dBm)
Addon 1	-13.45	-13.36	-13.25
Addon 2	-10.75	-12.94	-12.67

As can be seen in Figure 9 and Table 1, except for Addon 2, all other QSFPs exceeded the required -11 dBm specification for the QSFPs. This validates the compatibility of all FS and Vitex QSFPs with the X2O system when tested with the ME0 interface. The Addon QSFPs were seen to be comparatively worse than the FS and Vitex QSFPs and were not used for any further testing.

The Vitex QSFPs tended to have better sensitivity measurements than the FS ones, which indicates that they work with lower optical power signals and are therefore preferred for the use in the backend system. Based on these results, it was decided that Vitex would be used for all further experiments due to its better performance.

3.2 Frontend Interfaces

Three frontend interfaces were tested with the QSFPs to determine compatibility with the X2O system: the ME0, GE2/1, and DMB frontend muon interfaces. Figure 10 shows a comparison of maximum sensitivities measured with all three interfaces. 32 Vitex QSFPs were tested using the ME0, 24 Vitex QSFPs were tested with the GE2/1, and 22 Vitex QSFPs were tested using the DMB. All three channels were combined into one plot for each interface to have a more significant sample size for comparison between the interfaces.

The ME0 system has a transmission speed of 10.24 Gbps, GE2/1 has 4.8 Gbps, and DMB has 1.6 Gbps. As can be seen from the plots, transmission speed affects the sensitivity measurements associated with each device: lower transmission speeds allow for better measurements. This is a result of the transmitted data having more of a time delay between each bit, allowing the receiver system more time to detect the optical signal which increases reliability.

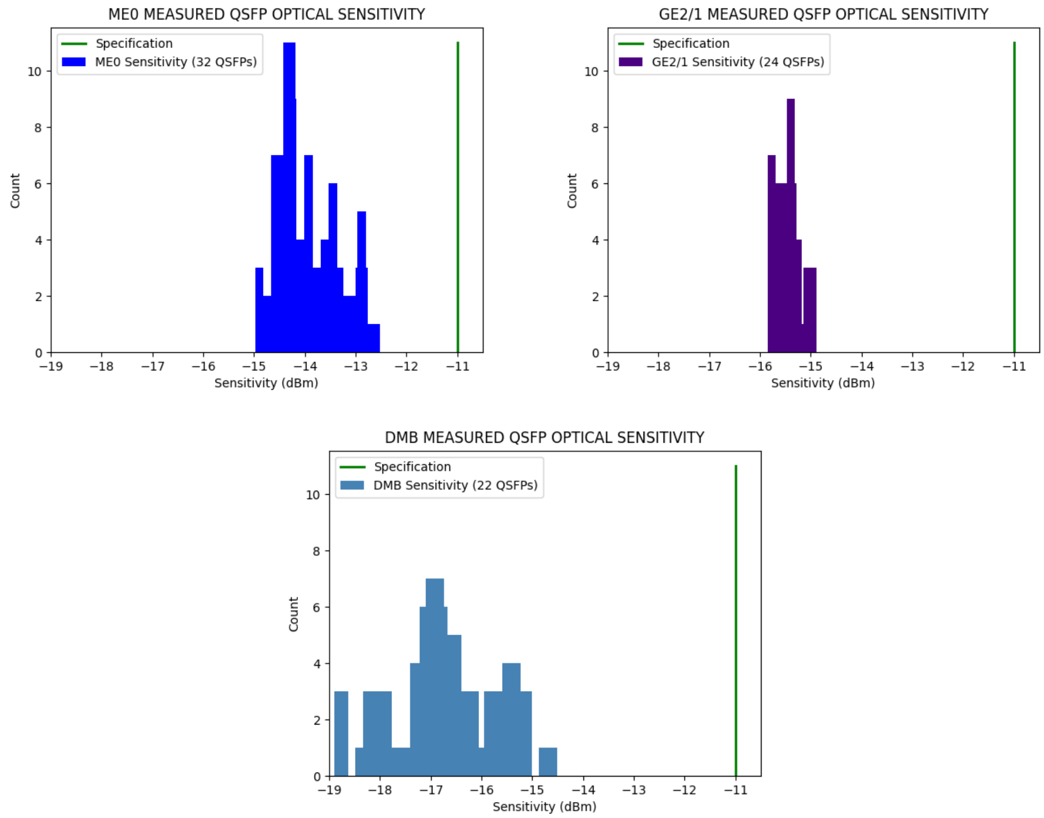

Figure 10: QSFP sensitivity measurements with ME0, GE2/1, and DMB, all channels included

In addition to Figure 10 above, Figures 11-13 below show the three different channels for each of the interfaces, using 32, 24, and 22 Vitex QSFPs for the ME0, GE2/1, and DMB, respectively:

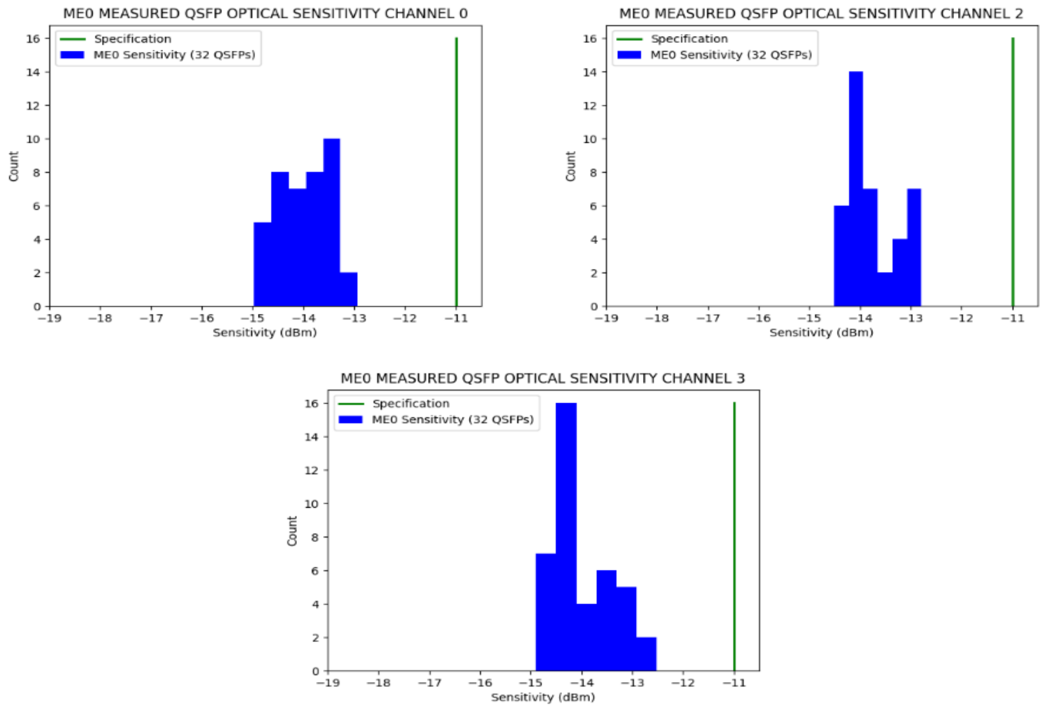

Figure 11: ME0 sensitivity measurements for channels 0, 2, and 3

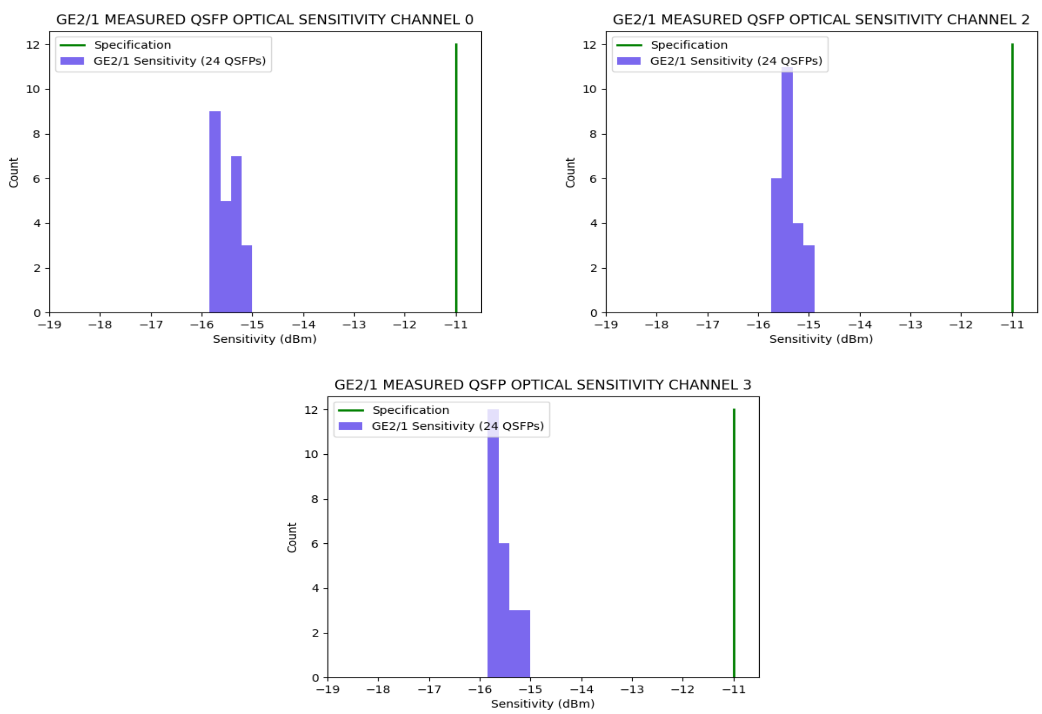

Figure 12: GE2/1 sensitivity measurements for channels 0, 2, and 3

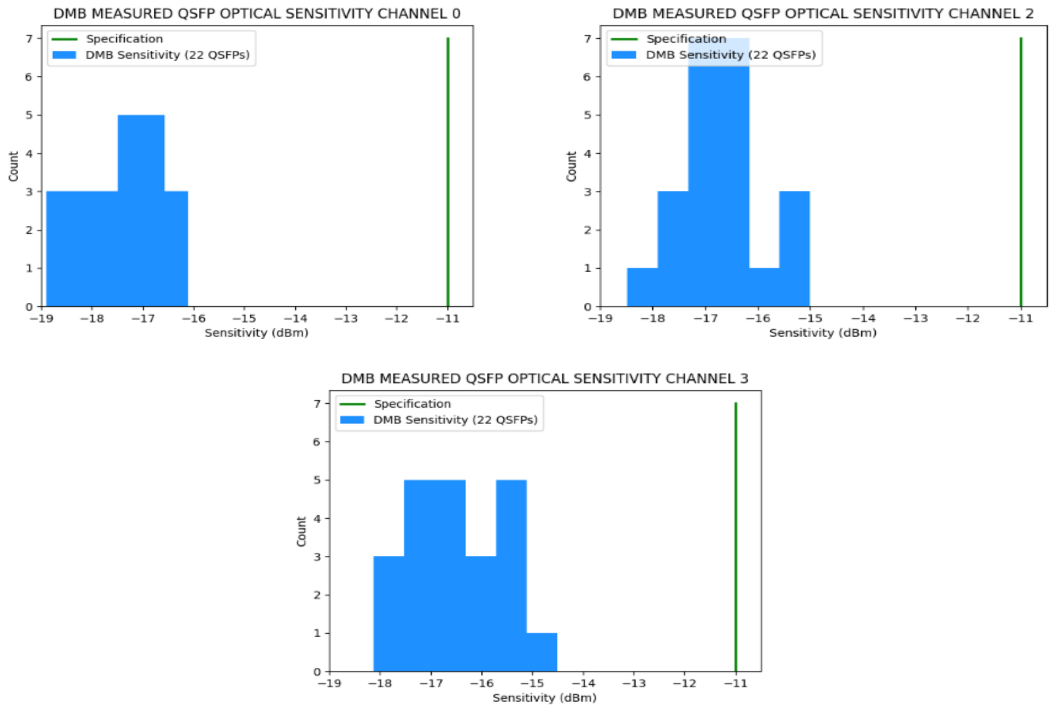

Figure 13: DMB sensitivity measurements for channels 0, 2, and 3

Figures 11, 12, and 13 show the sensitivity measurements of channels 0, 2, and 3 for the ME0, GE2/1, and DMB interfaces, respectively. As can be seen from the figures, the measurements in each channel of the same interface are somewhat consistent, but have a small variation from each other. The average optical sensitivity and standard deviation of each channel is summarized in Table 2 below.

Table 2: Comparison of mean optical sensitivity of each channel, and the total mean and standard deviation of all channels, using the ME0, GE2/1, and DMB interfaces

Optical Sensitivity	Channel 0 mean (dBm)	Channel 2 mean (dBm)	Channel 3 mean (dBm)	Total mean (dBm)	Standard deviation (dBm)
ME0	-14.1	-13.7	-14.0	-13.9	0.6

GE2/1	-15.5	-15.4	-15.6	-15.5	0.3
DMB	-17.4	-16.7	-16.5	-16.9	1.0

As can be seen again from Table 2, each interface has a different range of optical receiver sensitivity measurements due to their different transmission speeds. Additionally, there are variations between all three channels when using the same interface. These variations are not very significant, but are more noticeable using the DMB from the given statistics. Each channel mean falls within one standard deviation away from the total mean sensitivity of each interface, and all deviations between channels are within expectation.

These differences could be potentially explained by chip-to-chip variation between the internal components of each QSFP due to their mass production by the manufacturer. Another possible explanation is that the amount of light leaking from each channel is different, causing a slightly different sensitivity measurement for each channel. A third explanation is that there could be small amounts of dust on some of the fiber connections, which would absorb different amounts of the incoming light and create differences in sensitivity.

3.3 RX Squelch

Optical receiver (RX) squelch is a manufacturer-installed feature on the QSFP transceivers that automatically stops transmission when the signal's optical power is too low. This setting can interfere with the experiments performed, because when the attenuation of the fiber is high enough, the QSFPs immediately stop operation; this prevents the optical power from reaching as low as it could without this RX squelch feature in place.

The Vitex QSFPs have two more advantages compared to the FS QSFPs tested earlier: the Vitex QSFP RX squelch threshold is much lower, at around -15 dBm compared to -10 dBm for the FS parts, allowing further operation under weak optical signals; and more importantly, the RX squelch is a programmable feature on the Vitex transceivers that can be disabled with a simple command issued through the X2O, something which the FS transceivers were not capable of.

Figure 14 shows the sensitivity measurements of all three channels of QSFPs tested with the DMB interface, with the orange sample having RX squelch enabled and the blue sample having RX squelch disabled.

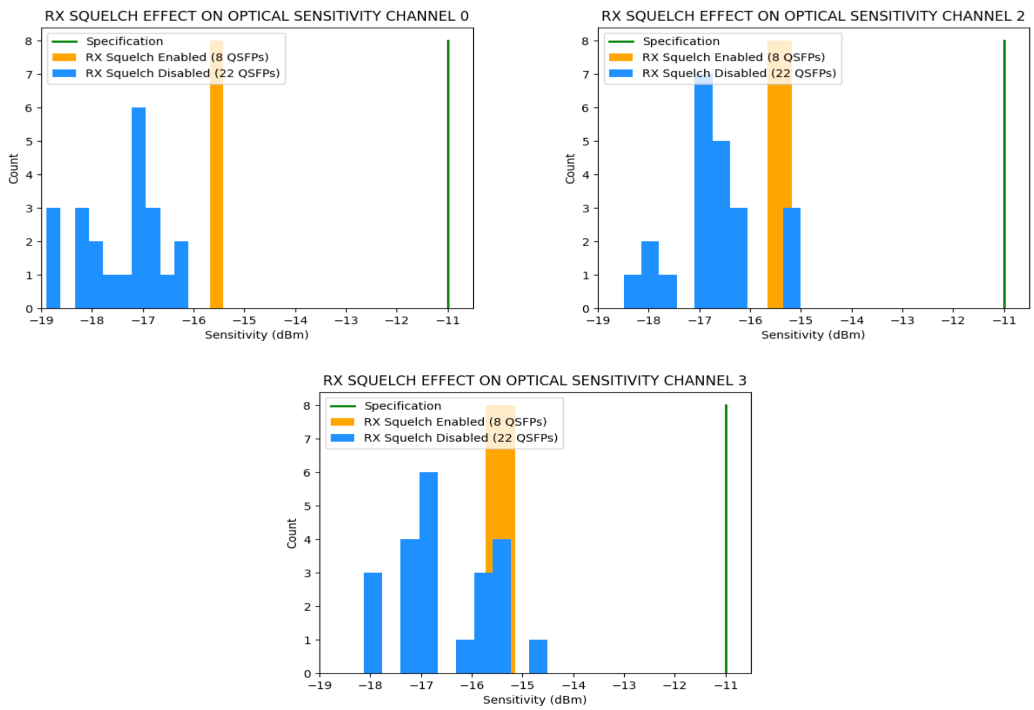

Figure 14: Effects of RX squelch on optical sensitivity

As can be seen in Figure 14, disabling the RX squelch generally improved the sensitivity measurements of the QSFPs. The average of all three channels was -15.46 dBm with RX squelch enabled and -16.87 dBm with RX squelch disabled. This proved that the RX squelch feature was effective in improving the performance of the QSFPs, and could even improve performance by more than 1 dBm difference.

Further testing showed that disabling the squelch was more effective in the interface systems with slower transmission speeds, such as the DMB and GE2/1, while not as effective with the ME0 interface, which is much faster. In Table 3 below, a comparison is shown for the DMB, GE2/1, and ME0 interfaces to show the difference between the RX squelch feature being enabled and disabled, with the measurement being an average of all three channels on one Vitex QSFP.

Table 3: Comparison of RX squelch enabled and disabled for the ME0, GE2/1, and DMB interfaces. Sensitivity measurements are taken as an average of all three channels for one QSFP.

Average RX Squelch Sensitivity	Squelch Enabled (dBm)	Squelch Disabled (dBm)
ME0	-13.25	-13.20
GE2/1	-15.2	-16.96
DMB	-15.67	-18.54

The ME0 interface had no significant change between the two settings, with the difference being within the expected random variation in sensitivity results. The GE2/1 and DMB interface showed significant differences in the measured sensitivities, on the order of 1.7 and 1.9 dBm in this case, respectively.

After the RX squelch feature could be disabled on the Vitex QSFPs, it was left disabled for all further testing of these QSFPs due to its improvement to their performance.

3.4 Forward Error Correction

Forward Error Correction (FEC) is a feature present in the GEM type interfaces, used for correction of bitstream errors that occur during transmission. The FEC feature is capable of correcting a single bit error at a time which may happen occasionally, as well as detecting multiple bit errors that may occur all at once. As a result, post-FEC reliability is generally improved over pre-FEC uncorrected data.

While testing QSFP sensitivities using the ME0 and GE2/1, this FEC feature was used to correct some of the bit errors during this test. Most of the testing performed during this research with these two interfaces was done by checking the number of errors after they have been corrected. To see the difference between maximum sensitivity results when considering the FEC feature, 10 different Vitex QSFPs were measured with the ME0 system with and without taking into account FEC.

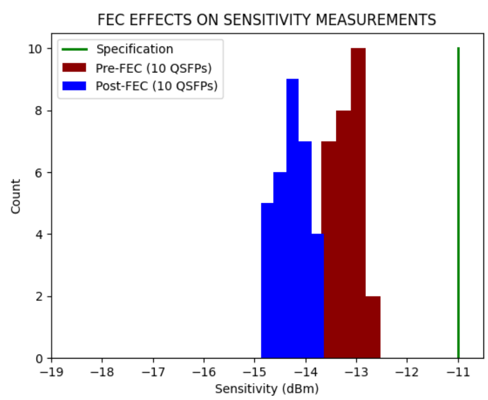

Figure 15: Sensitivity measurements of Vitex QSFPs using the ME0, with and without taking into account Forward Error Correction

In Figure 15, the pre-FEC results are the measurements taken without FEC taken into consideration for maximum sensitivity, and the post-FEC results are those with FEC taken into consideration. The average of the pre-FEC result was -13.27 dBm and the average of the post-FEC result was -14.25 dBm, meaning that the FEC feature improved the maximum optical sensitivity of the QSFPs by about 1 dBm.

3.5 ME0 ASIAGO Board Testing

ME0 ASIC and Gigabit Optics (ASIAGO) [9] boards are electronic chips present on the ME0 detector interface, which are capable of sending data from the detector through optical fibers. In this research project, these boards are responsible for transmitting data from the ME0 to the X2O board.

All testing performed with the ME0 has used one specific ASIAGO board, numbered 8. However, three additional boards arrived for testing, which prompted a new test of switching the used ASIAGO board and comparing their results with one specific QSFP to ensure that all boards have a consistent level of signal output.

The following table shows a comparison between the ASIAGO used for most testing – number 8 – and the three other boards, numbered 5, 6, and 7. The table is ordered following the testing order of the boards.

Table 4: Optical receiver sensitivities using four different ASIAGO boards belonging to the ME0 interface. Values given in the table are individual measurements.

ASIAGO board optical sensitivity	Channel 0 (dBm)	Channel 2 (dBm)	Channel 3 (dBm)
ME0 ASIAGO #8	-14.3	-14.01	-14.5
ME0 ASIAGO #7	-14.34	-13.93	-14.01
ME0 ASIAGO #6	-13.82	-13.08	-13.34
ME0 ASIAGO #5	-13.43	-12.79	-12.77

Initially, the results seemed to differ from each other by significant margins of around 1 dBm difference each, and as testing progressed the boards tested seemed to have worse results than before. However, this actually turned out to be caused by dust accumulating on the fiber optical connection; upon cleaning the fibers, ASIAGO #5 showed expected results:

	Channel 0 (dBm)	Channel 2 (dBm)	Channel 3 (dBm)
ME0 ASIAGO #5	-14.29	-14.09	-13.87

All ASIAGO boards for the ME0 showed similar power readings, within the expected deviation between different sensitivity readings. This indicates that they all have the same power output, which won't cause problems in the CMS experiment when used on ME0 boards.

3.6 QSFP Retesting

Retesting of QSFPs was conducted to ensure that performance results would not greatly vary with time. Two different methods were used to confirm this: a couple of QSFPs were retested once after their original test to compare sensitivity measurements, and of those a few chosen QSFPs were retested multiple times over a longer period of time.

As can be seen from Figure 16, 8 Vitex QSFPs were retested with the ME0, 2 months after their initial testing. The average of all three channels was taken for the measurement of each QSFP.

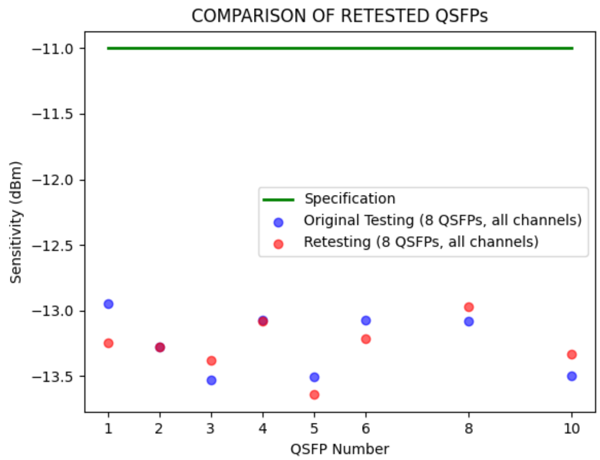

Figure 16: Retesting of 8 chosen Vitex QSFPs with ME0, 2 months after original testing

After retesting, it was observed that the retested QSFPs had similar sensitivities to their original measurement and were all within the expected range of difference in measurement due to randomness of the configuration of the fiber connection. This confirmed that the TAMU optical testing system did not deteriorate over time, and that there would not be a lot of randomness involved in retesting of QSFPs. This leads to the conclusion that sensitivity measurements stayed consistent over the testing period while using the test stand at the Texas A&M electronics lab.

4. CONCLUSION

The goal of the testing performed in this research experiment is to verify compatibility of these QSFP transceivers with the X2O board. For this purpose, an automated optical test stand was built at the TAMU CMS electronics lab and software was written to control all components of the test stand.

Test specifications were created to qualify compatibility of the QSFPs with the X2O and the various frontend interfaces tested.

The testing performed during this research involved extensive measurements of the sensitivities of all QSFPs – which included testing of three different types of QSFPs from three manufacturers, testing of QSFPs with three frontend muon interfaces of different transmission speeds, and testing with various features such as the forward error correction and RX squelch.

The QSFPs tested with the ME0, GE2/1, and DMB interfaces all proved to satisfy the requirements for compatibility. This ensures they can be reliably used with these interfaces at the CMS experiment in the LHC. Additionally, since the QSFPs tested proved compatible with the DMB, one of the interface devices with the lowest transmission speed, these QSFPs will also likely be compatible with other GEM and CSC interfaces used in the CMS experiment but not tested during this research project.

QSFPs from two different manufacturers, FS and Vitex, were measured and compared; Vitex QSFPs proved to have better sensitivity measurements and features that were more suitable for use in the CMS experiment. These Vitex QSFPs were then used for the rest of the experimentation performed in this research project.

RX squelch, a built-in feature that inhibits QSFP performance, was also discovered during this research. It was found that this feature could be disabled for Vitex QSFPs only by using programmable settings. Disabling this feature proved that the sensitivity results could be improved even further, allowing reliable data transmission with even weaker optical signals.

All of these measurements were used to verify QSFP compatibility with the backend muon system of the CMS experiment, namely the X2O board, as well as the various GEM and CSC detector interfaces that collect muon data and communicate with the X2O. This proves their suitability for use in the High-Luminosity LHC upgrade to the CMS experiment as high-speed transmission devices that will be able to handle the muon data reliably.

REFERENCES

[1] Technical design report, CERN Document Server. (1998). https://cds.cern.ch/record/343814 (accessed January 22, 2023).

[2] A. Lopes, M.L. Perrey, FAQ-LHC the guide, CERN Document Server. (2022). https://cds.cern.ch/record/2809109 (accessed January 22, 2023).

[3] The standard model, CERN. (n.d.). https://home.cern/science/physics/standard-model (accessed January 22, 2023).

[4] V.T. S., Beyond the standard model of particle physics, Philosophical Transactions of the Royal Society A: Mathematical, Physical and Engineering Sciences. (2016). https://royalsocietypublishing.org/doi/10.1098/rsta.2015.0259 (accessed January 22, 2023).

[5] High-luminosity LHC, CERN. (n.d.). https://home.cern/science/accelerators/high-luminosity-lhc (accessed January 15, 2023).

[6] Datasheet QSFP+ ESR4 - vitextech.com, (n.d.). https://vitextech.com/wp-content/uploads/2019/12/VQ-40SR4CP-EA.pdf (accessed January 19, 2023).

[7] 2: Layout of the LHC accelerator. the four large LHC experiments (Atlas ..., (n.d.). https://www.researchgate.net/figure/Layout-of-the-LHC-accelerator-The-four-large-LHC-experiments-ATLAS-CMS_fig1_48410628 (accessed February 27, 2023).

[8] CERN accelerating science, Detector | CMS Experiment. (n.d.). https://cms.cern/detector (accessed February 27, 2023).

[9] A. Peck, E. Juska, ME0 Electronics Prototypes Preliminary Testing Results, Indico. (2019). https://indico.cern.ch/event/847049/contributions/3583582/attachments/1919032/3173842/20191 (accessed March 10, 2023).

[10] DOE explains...muons, Energy.gov. (n.d.). https://www.energy.gov/science/doe-explainsmuons (accessed March 25, 2023).

[11] Trigger MotherBoard (TMB), CMS. (n.d.). https://cmsdoc.cern.ch/cms/MUON/cscTrigger/html/CERN/striplct.html (accessed March 25, 2023).

[12] CERN accelerating science, Real Time Analysis with the CMS Level-1 Trigger | CMS Experiment. (n.d.). https://cms.cern/news/real-time-analysis-cms-level-1-trigger (accessed March 25, 2023).

[13] J. Hauser, Experience with trigger electronics for the CSC SYSTEM OF CMS, ResearchGate. (2004). https://www.researchgate.net/publication/228524091_Experience_with_Trigger_Electronics_for_the_CSC_System_of_CMS (accessed March 30, 2023).

[14] Fs, CISCO QSFP-40G-SR4 compatible 40GBASE-SR4 QSFP+ transceiver module, FS.com. (n.d.). https://www.fs.com/products/36157.html (accessed March 30, 2023).

[15] N. Neumeister, Muon Short Exercise, Twiki. (2020). https://twiki.cern.ch/twiki/pub/CMS/SWGuideCMSDataAnalysisSchoolLPC2023MuonExercise/CMSDAS_LPC_Muons.pdf (accessed April 14, 2023).